Electronic Supplementary Material (ESI) for Organic & Biomolecular Chemistry

Electronic Supplementary Information for

Sulfur, Oxygen, and Nitrogen Mustards: Stability and Reactivity

*Qi-Qiang Wang, Rowshan Ara Begum, Victor W. Day, Kristin Bowman-James**

Department of Chemistry, University of Kansas, Lawrence, Kansas 66045

***Email: kbjames@ku.edu**

Contents

General experimental procedure

Figure S1. ^{1}H NMR changes of CEES in CD_3OD over time.

Figure S2. ^{1}H NMR changes of CEES in D_2O over time.

Figure S3. ^{1}H NMR changes of HN2 in DMSO-d_6 over time.

Figure S4. ^{1}H NMR changes of HN2 in CD_3OD over time.

Figure S5. ^{1}H NMR changes of HN2 in D_2O over time.

Figure S6. ^{1}H NMR changes of HN3 in DMSO-d_6 over time.

Figure S7. ^{1}H NMR changes of HN3 in CD_3OD over time.

Figure S8. ^{1}H NMR changes of HN3 in D_2O over time.

Figure S9. ^{1}H NMR monitoring of the reaction between BCEE and $(CH_3)_3N$ in $CDCl_3$ (with ESI-MS data).

Figure S10. ^{1}H NMR monitoring of the reaction between CEES and $(CH_3)_2NH$ in $CDCl_3$.

Figure S11. ^{1}H NMR monitoring of the reaction between CEES and $(CH_3)_3N$ in $CDCl_3$ (with ESI-MS data).

Figure S12. ^{1}H NMR monitoring of the reaction between HN2 and CH_3NH_2 in $CDCl_3$.

Figure S13. ^{1}H NMR monitoring of the reaction between HN2 and $CH_3CH_2NH_2$ in $CDCl_3$.

Figure S14. ^{1}H NMR monitoring of the reaction between HN2 and $(CH_3)_2NH$ in $CDCl_3$ (with ESI-MS data).

Figure S15. ^{1}H NMR monitoring of the reaction between HN2 and $(CH_3CH_2)_2NH$ in $CDCl_3$ (with ESI-MS data).

Figure S16. ^{1}H NMR monitoring of the reaction between HN2 and $(CH_3)_3N$ in $CDCl_3$ (with ESI-MS data).

Figure S17. ^{1}H NMR monitoring of the reaction between HN3 and $(CH_3)_2NH$ in $CDCl_3$ (with ESI-MS data).

Figure S18. ^{1}H NMR monitoring of the reaction between HN3 and $(CH_3CH_2)_2NH$ in $CDCl_3$ (with ESI-MS data).

Figure S19. ^{1}H NMR monitoring of the reaction between HN3 and $(CH_3)_3N$ in $CDCl_3$ (with ESI-MS data).

Figure S20. ^{1}H NMR of the precipitates isolated from the reaction between BCEE and $(CH_3)_2NH$ in $CDCl_3$ (with ESI-MS data).

Figure S21. ^{1}H NMR of the precipitates isolated from the reaction between HN3 and CH_3NH_2 in $CDCl_3$ (with ESI-MS data).

Table S1. Crystallographic data for 4,4-dimethylmorpholinium chloride (**A**) and 2,2'-oxybis(*N*,*N*,*N*-trimethylethanaminium) dichloride (**B**).

General experimental procedure

Oxygen mustard, bis(β-chloroethyl) ether (BCEE), and half mustard, 2-chloroethyl ethyl sulfide (CEES) were purchased from Aldrich and used as received. Nitrogen mustards HN2 and HN3 were purchased from Aldrich and received as hydrochloride form, mechlorethamine hydrochloride and tris(2-chloroethyl)amine hydrochloride. The hydrochloride was neutralized by NaOH in water and extracted rapidly with diethyl ether, dried over anhydrous Na_2SO_4 to give the free amine form. Deuterated solvents $CDCl_3$, CD_3CN, DMSO-d_6, CD_3OD and D_2O were purchased from Cambridge Isotope Laboratories, Inc. Nuclear magnetic resonance (NMR) spectra were recorded on a Bruker Avance 400 spectrometer. Chemical shifts of the protons are expressed in ppm and calibrated against TMS as an internal reference or the residue solvent proton signals. Mass spectral data were obtained from the Mass Spectrometry Laboratory at the University of Kansas on a LCT Premier Mass spectrometer.

For X-ray crystallography study, intensity data were collected at 100K using a Bruker APEX II CCD area detector mounted on a Bruker D8 goniometer. Monochromatic Cu K_α radiation (λ = 1.54178 Å) was provided with Helios multilayer optics and a Bruker MicroStar microfocus rotating anode operating at 45kV and 60mA. The crystallographic data and details of data collection for 4,4-dimethylmorpholinium chloride (**A**) and 2,2'-oxybis(*N*,*N*,*N*-trimethylethanaminium) dichloride (**B**) are given in Table S1.

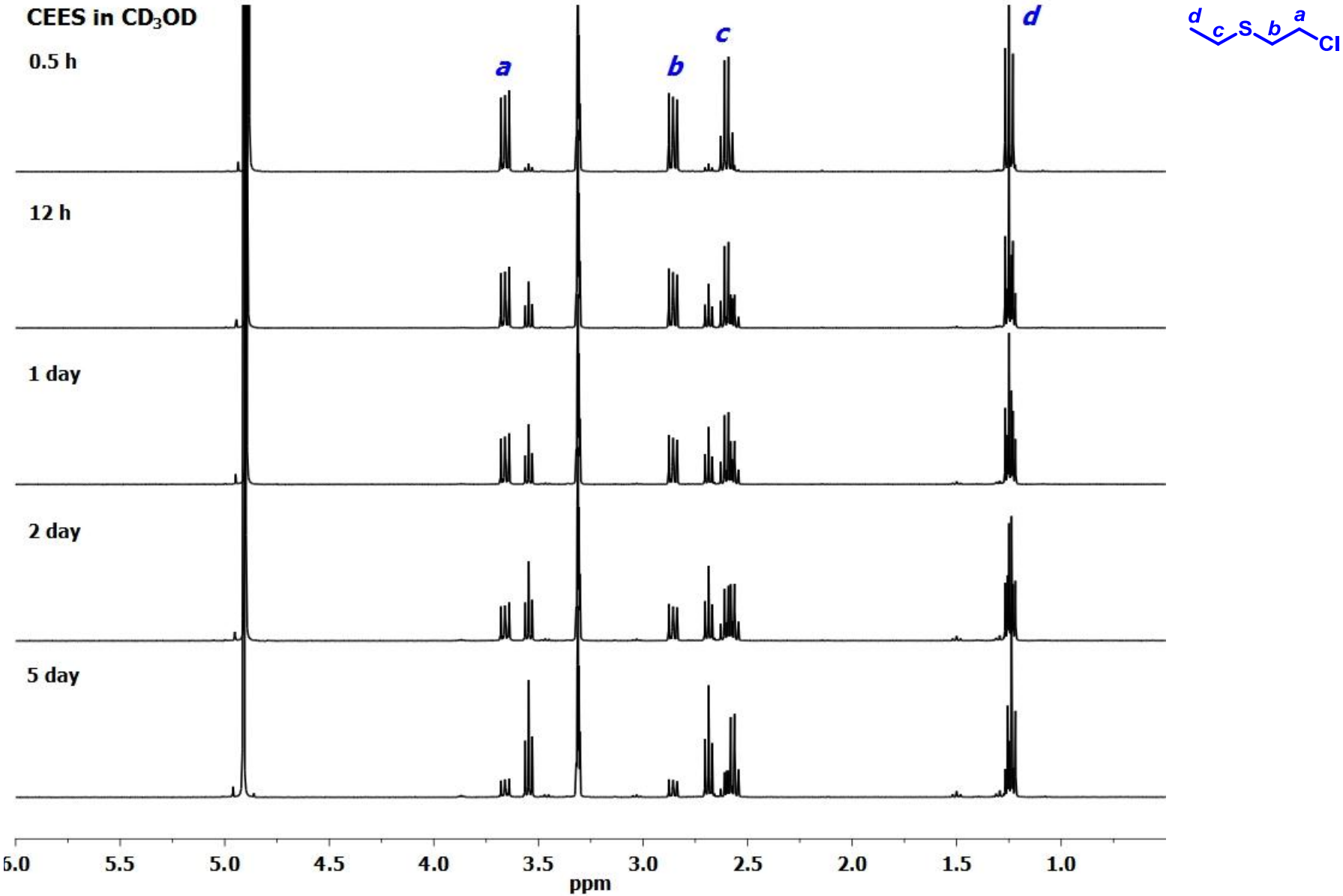

Figure S1. [1] H NMR changes (400 MHz, rt) of CEES in CD_3OD over time.

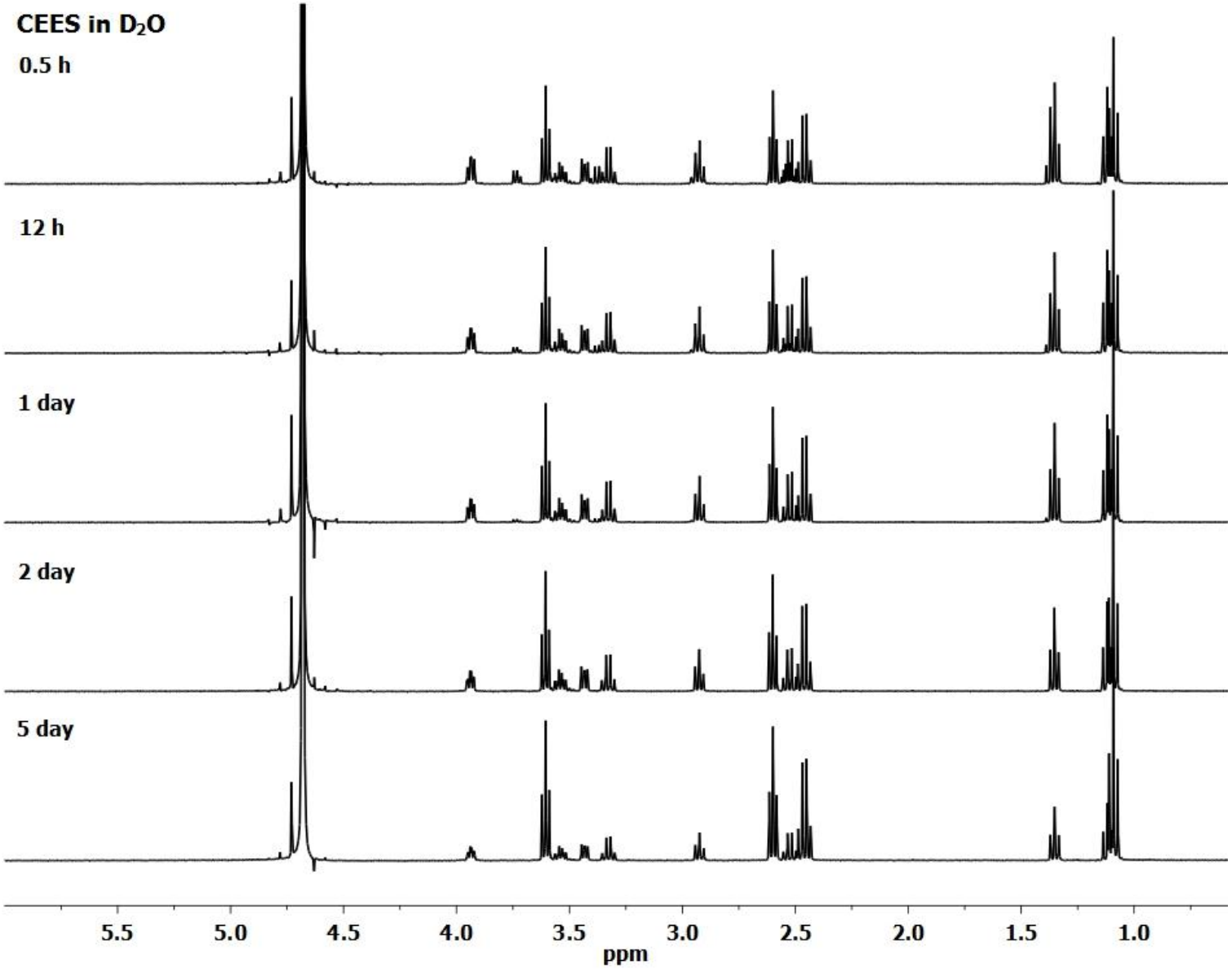

Figure S2. ^{1}H NMR changes (400 MHz, rt) of CEES in D_2O over time.

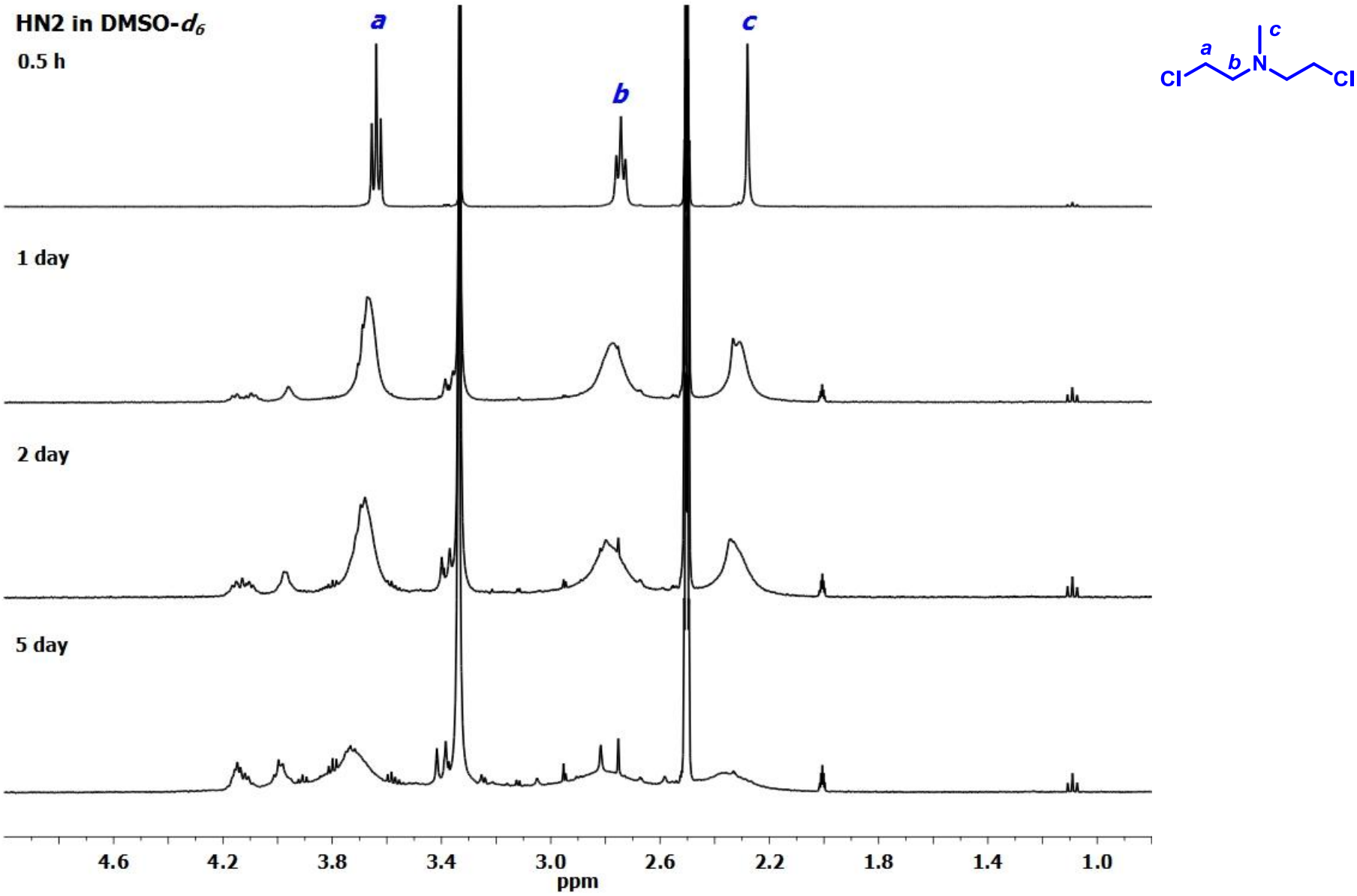

Figure S3. [1] H NMR changes (400 MHz, rt) of HN2 in DMSO-d_6 over time.

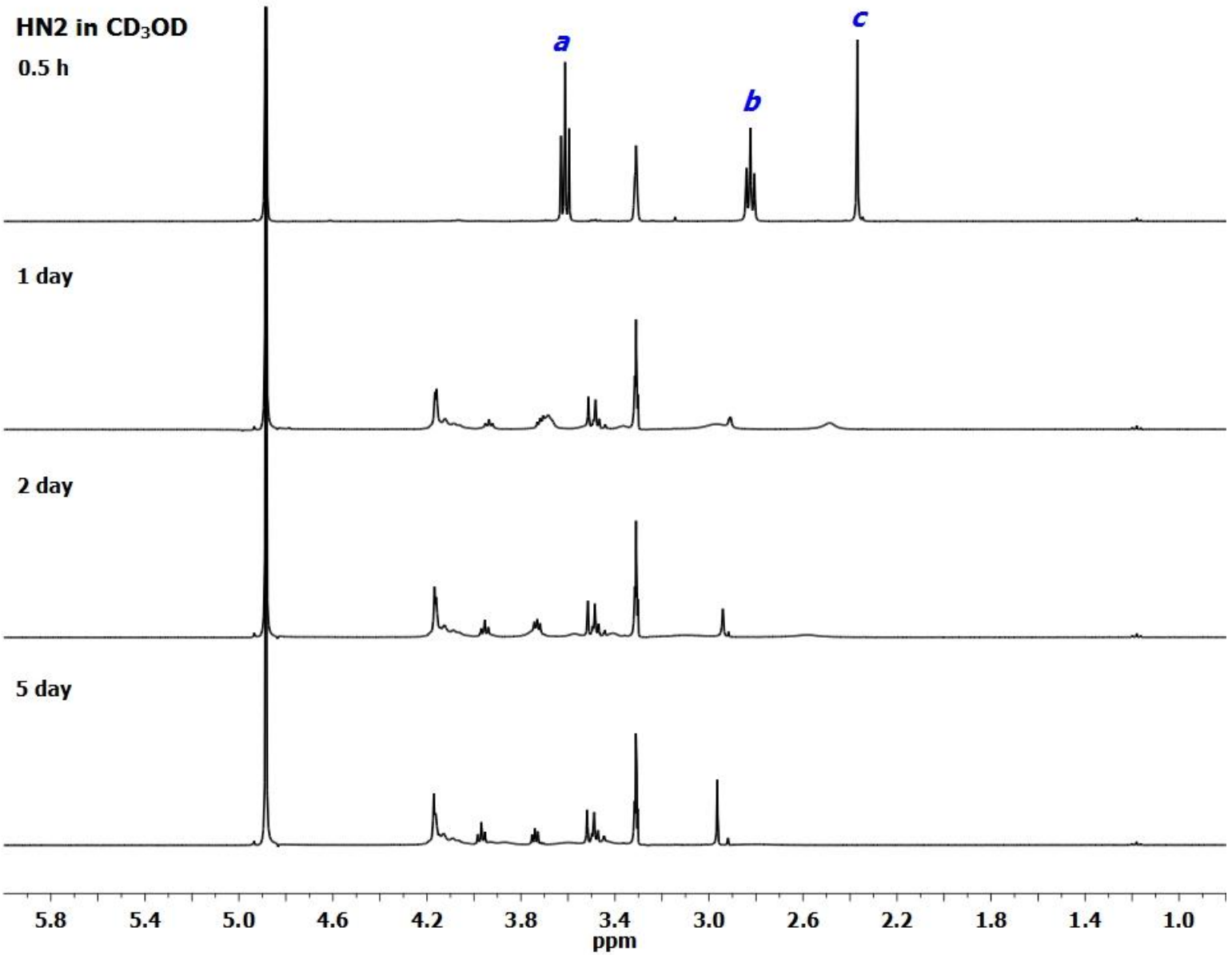

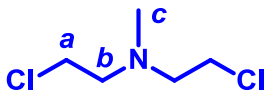

Figure S4. [1] H NMR changes (400 MHz, rt) of HN2 in CD_3OD over time.

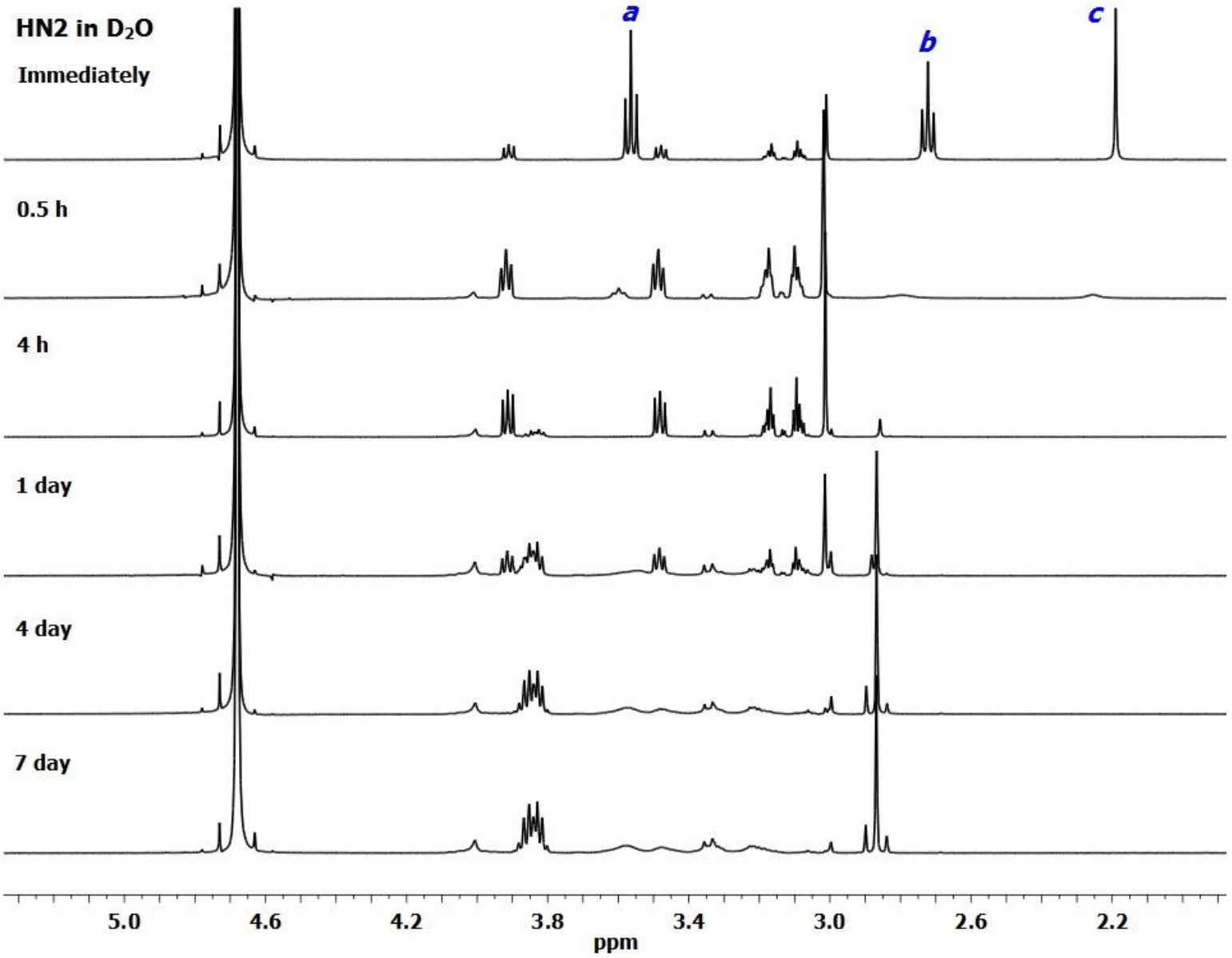

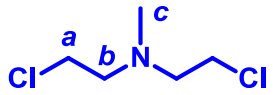

Figure S5. ^{1}H NMR changes of HN2 in D_2O over time.

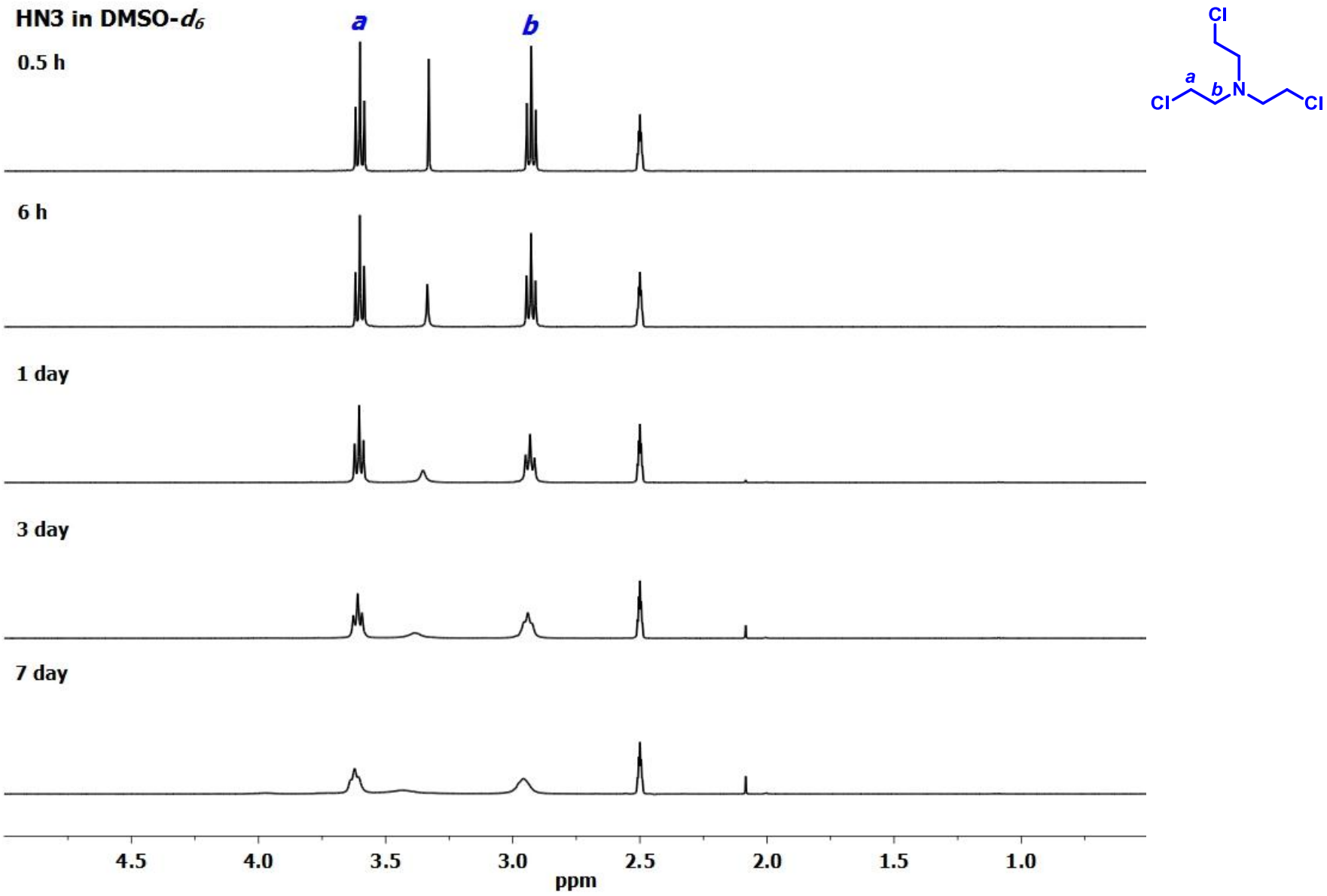

Figure S6. [1] H NMR changes (400 MHz, rt) of HN3 in DMSO-d_6 over time.

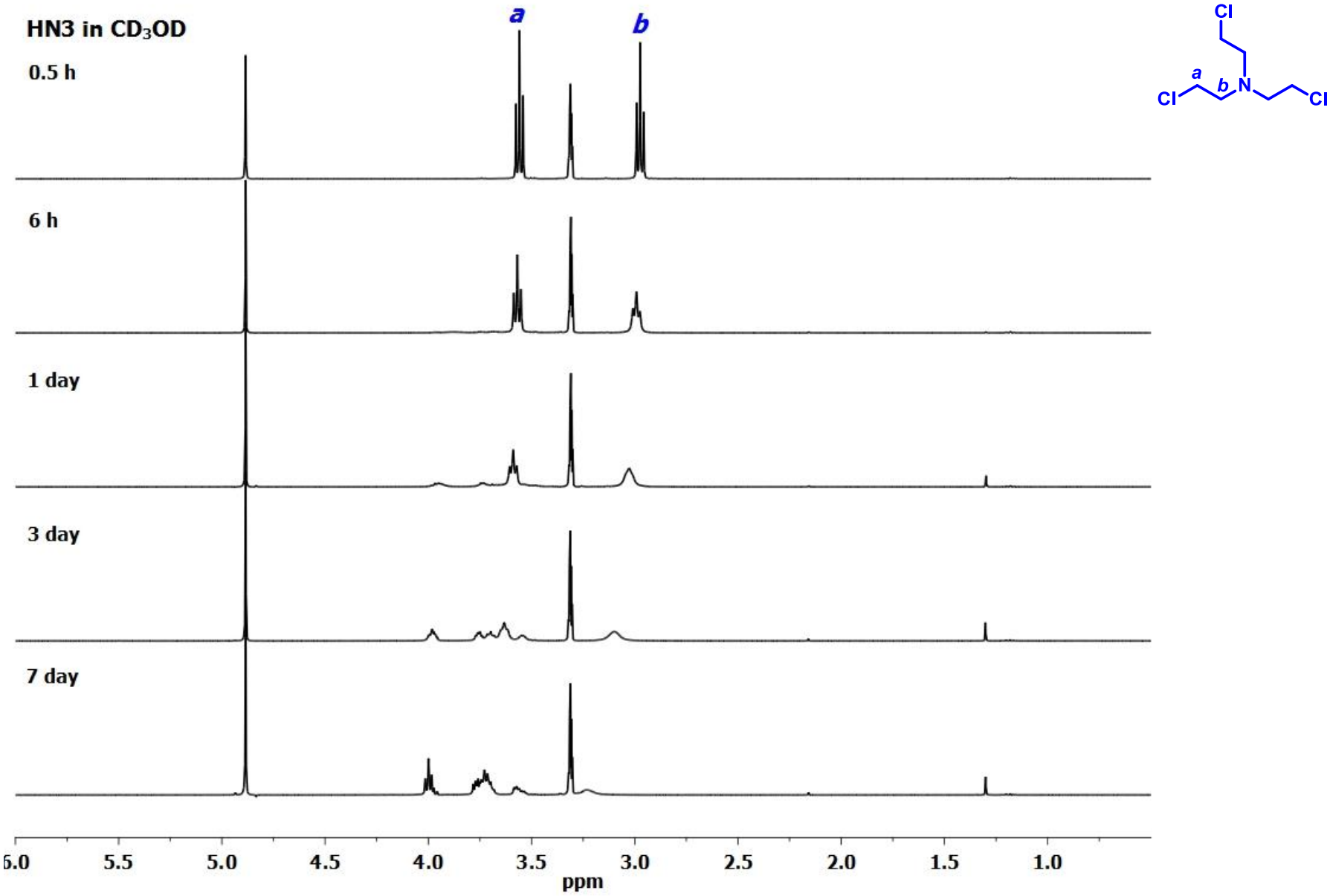

Figure S7. ^{1}H NMR changes (400 MHz, rt) of HN3 in CD_3OD over time.

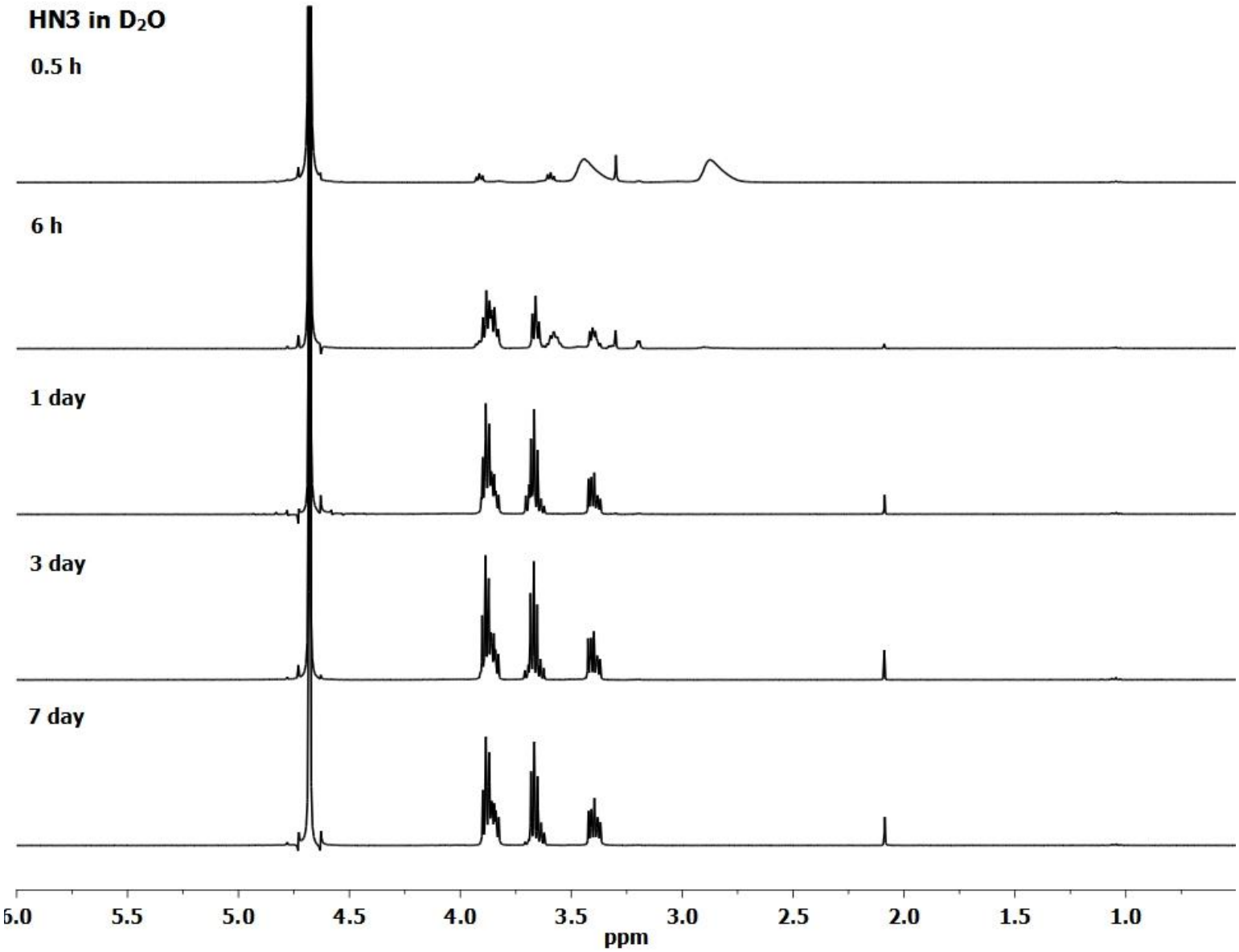

Figure S8. ^{1}H NMR changes (400 MHz, rt) of HN3 in D_2O over time.

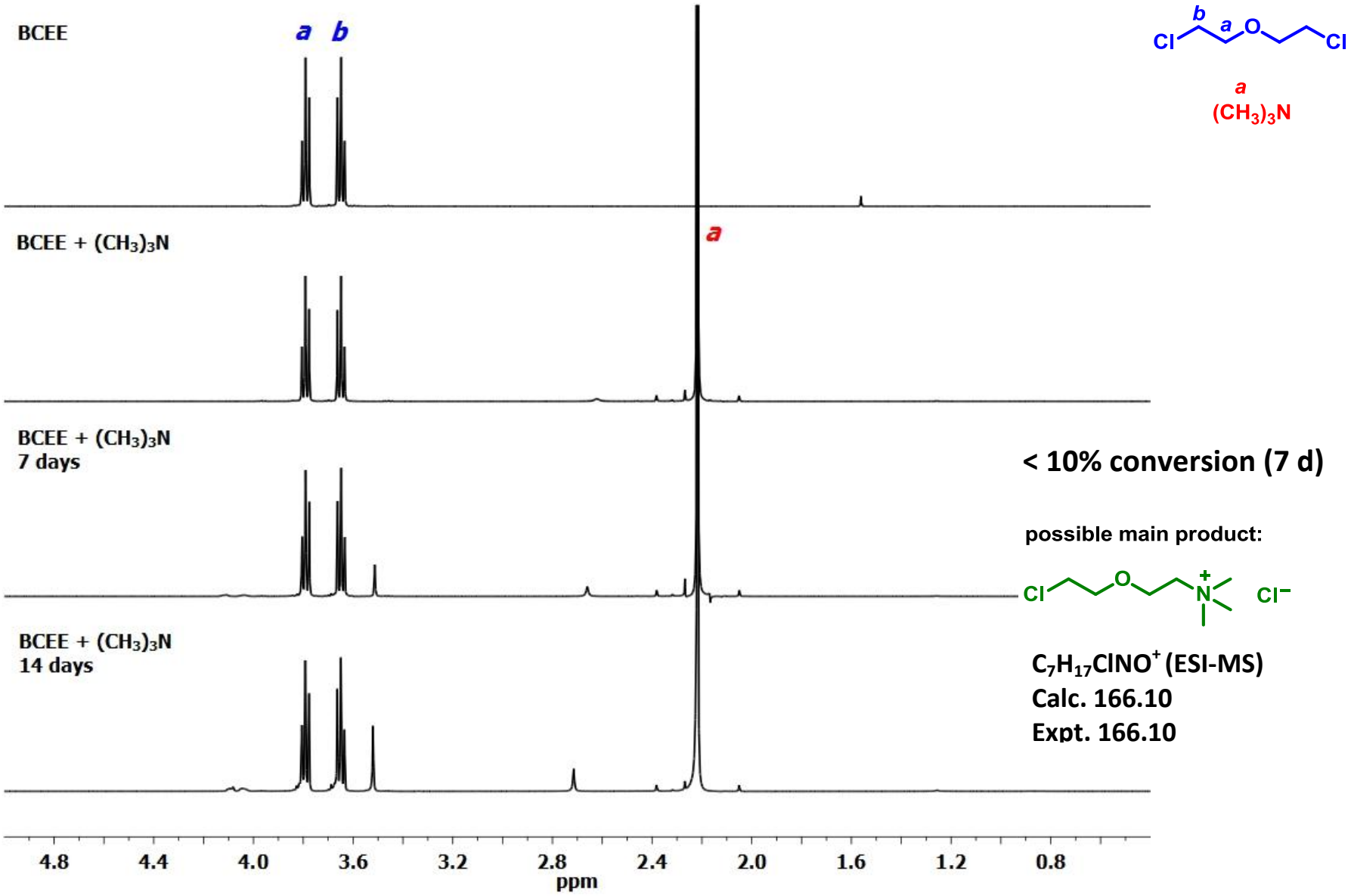

Figure S9. ^{1}H NMR monitoring (400 MHz, rt) of the reaction between BCEE and $(CH_3)_3N$ in $CDCl_3$ (with ESI-MS data).

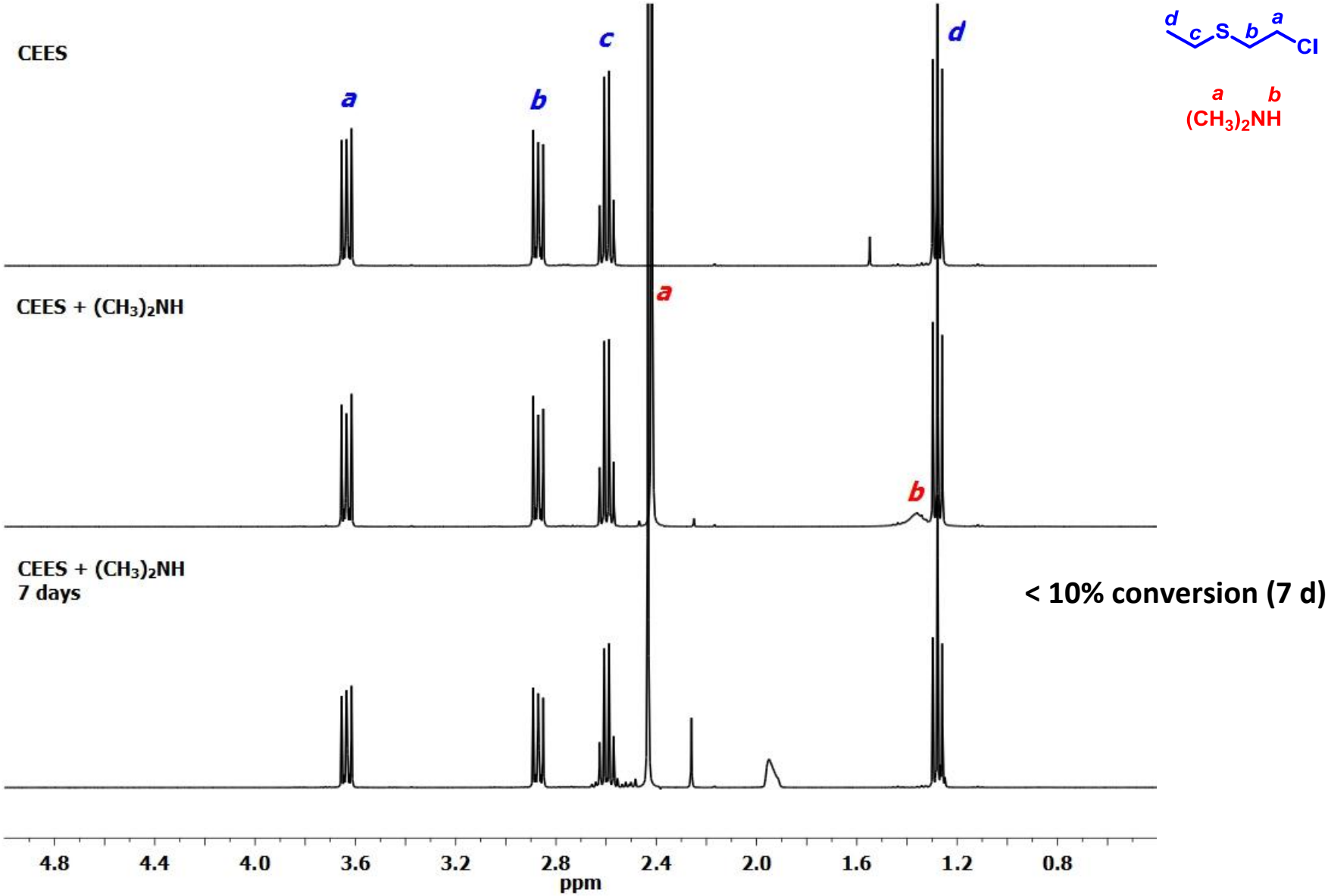

Figure S10. ^{1}H NMR monitoring (400 MHz, rt) of the reaction between CEES and $(CH_3)_2NH$ in $CDCl_3$.

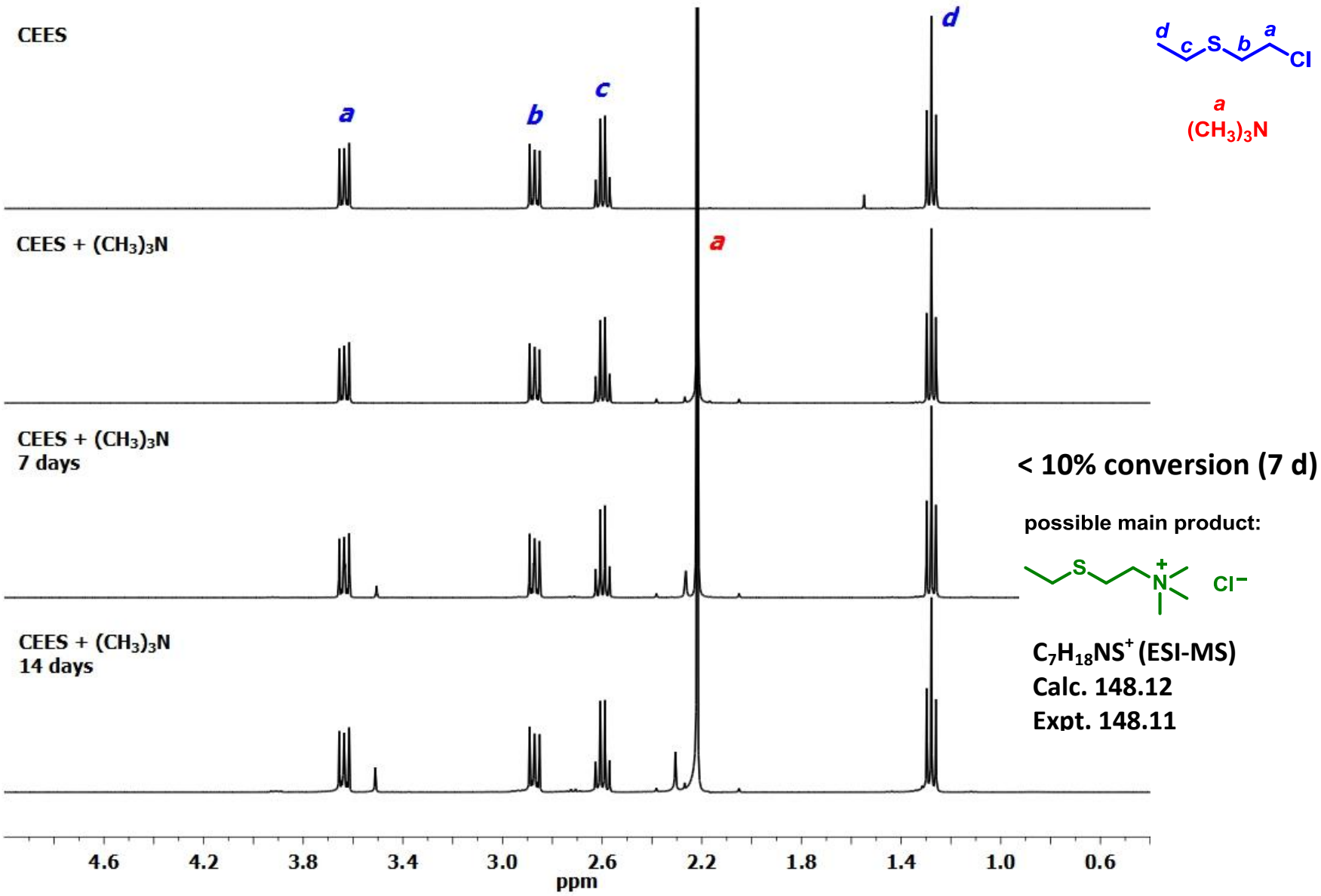

Figure S11. ^{1}H NMR monitoring (400 MHz, rt) of the reaction between CEES and $(CH_3)_3N$ in $CDCl_3$ (with ESI-MS data).

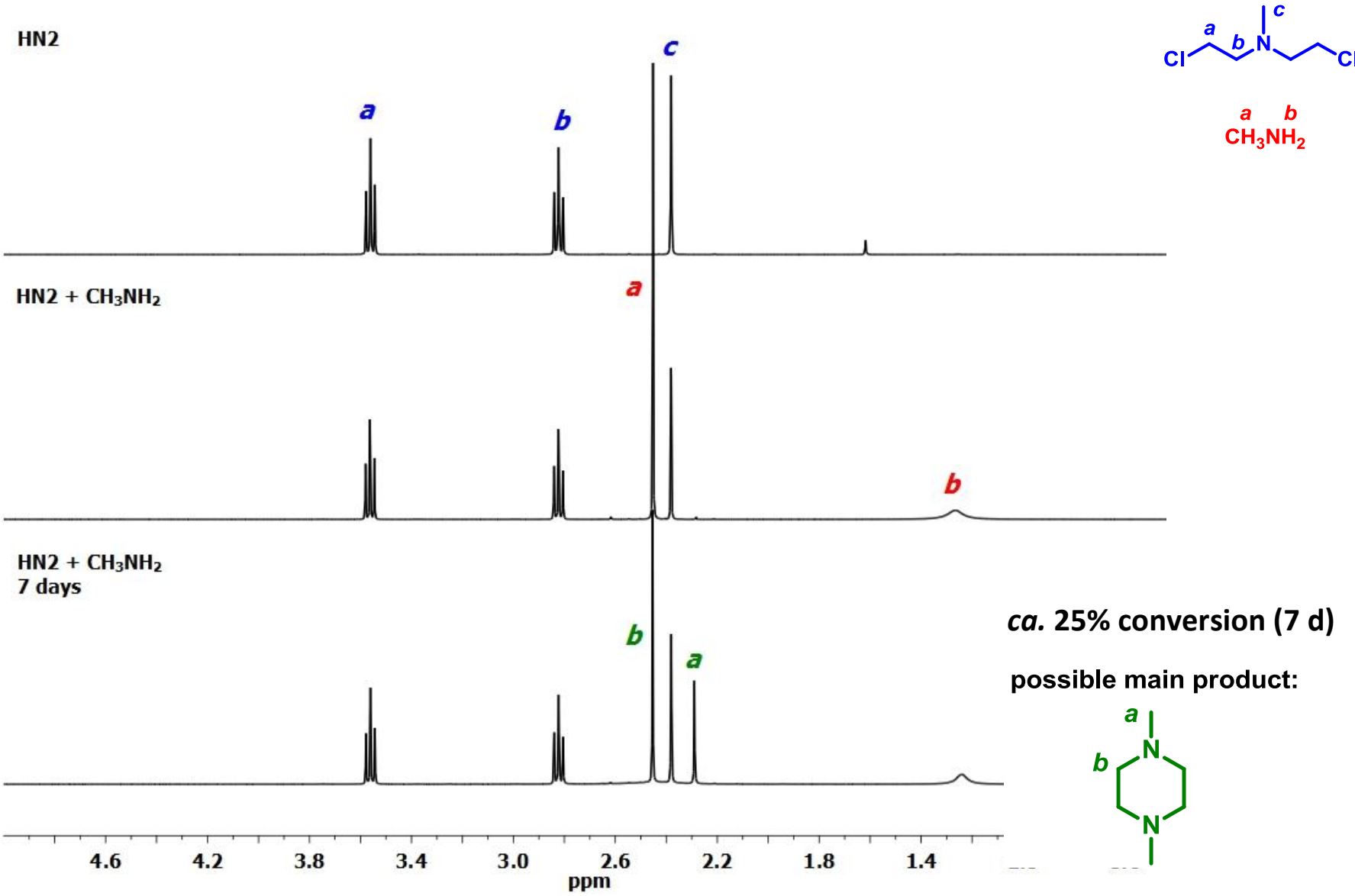

Figure S12. [1] H NMR monitoring (400 MHz, rt) of the reaction between HN2 and CH_3NH_2 in $CDCl_3$.

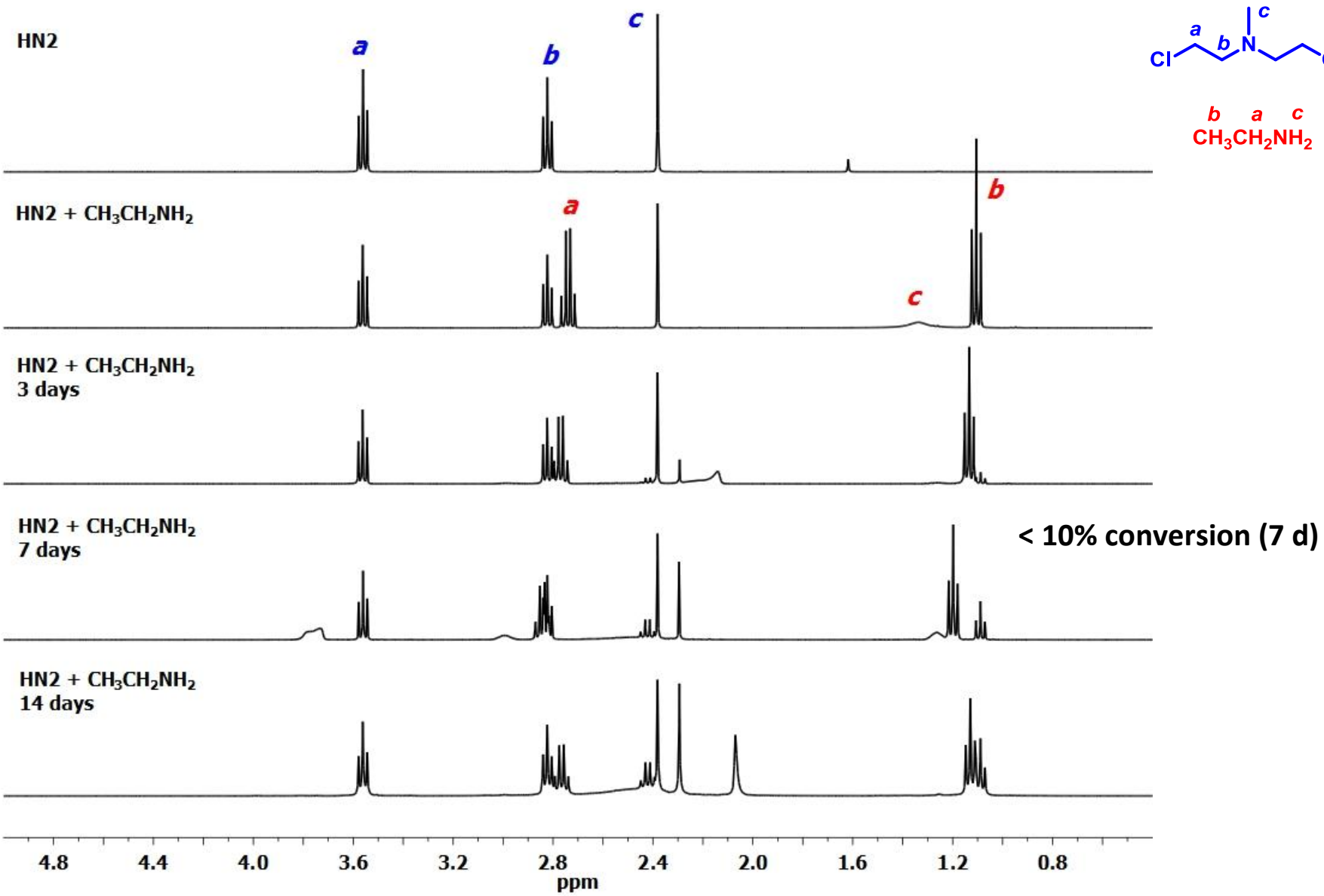

Figure S13. ^{1}H NMR monitoring (400 MHz, rt) of the reaction between HN2 and $CH_3CH_2NH_2$ in $CDCl_3$.

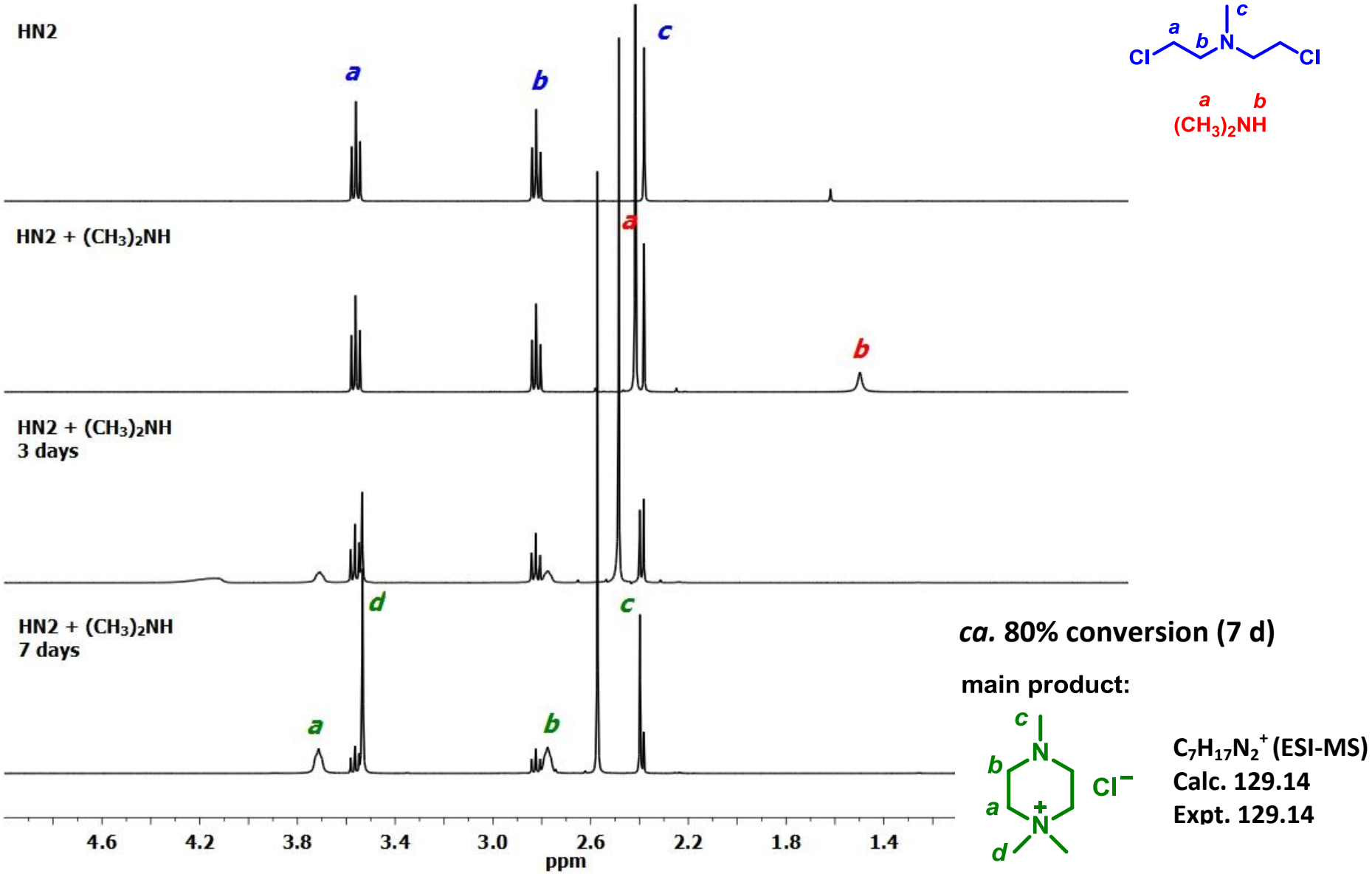

Figure S14. ^{1}H NMR monitoring (400 MHz, rt) of the reaction between HN2 and $(CH_3)_2NH$ in $CDCl_3$ (with ESI-MS data).

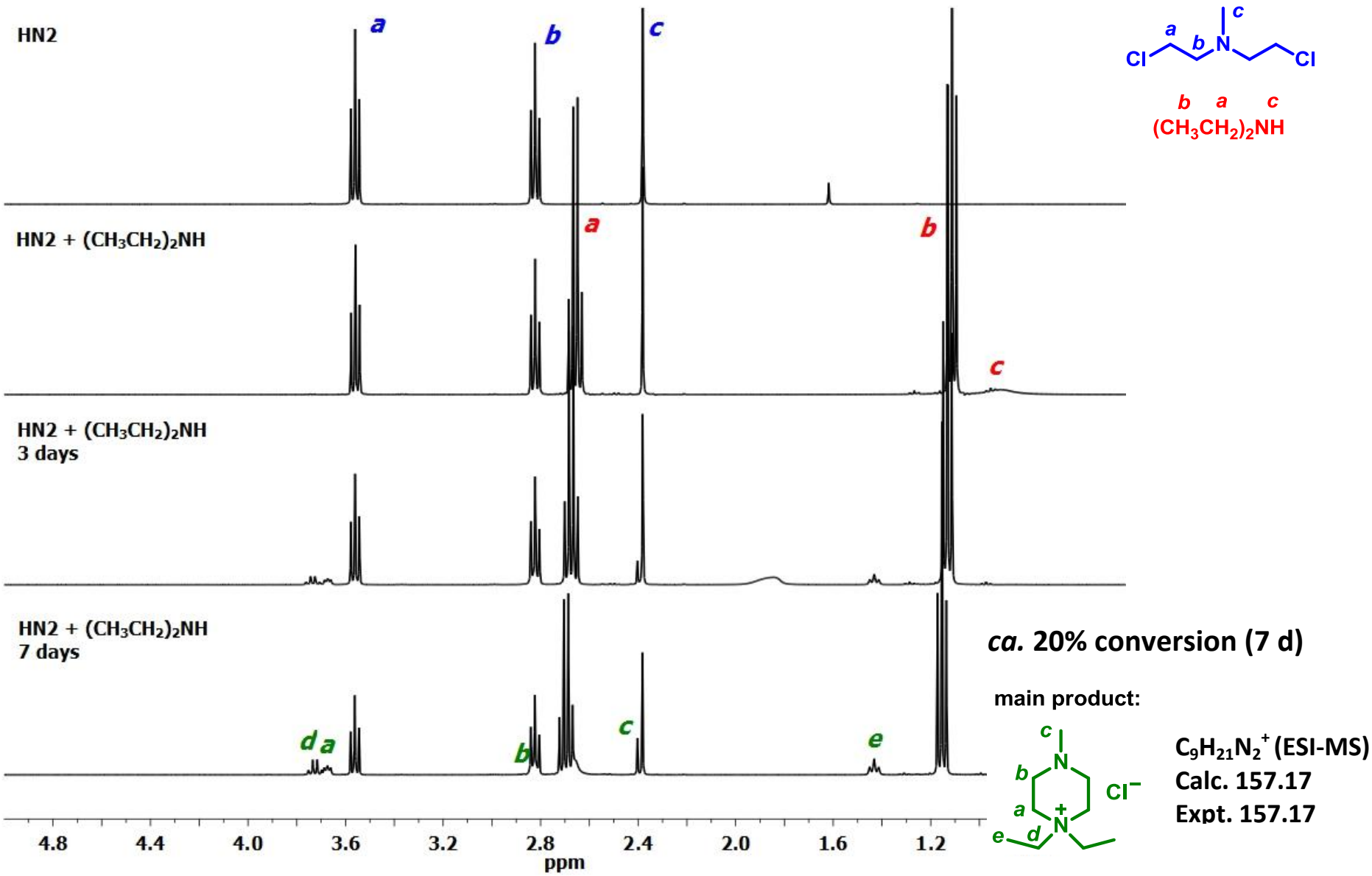

Figure S15. ^{1}H NMR monitoring (400 MHz, rt) of the reaction between HN2 and $(CH_3CH_2)_2NH$ in $CDCl_3$ (with ESI-MS data).

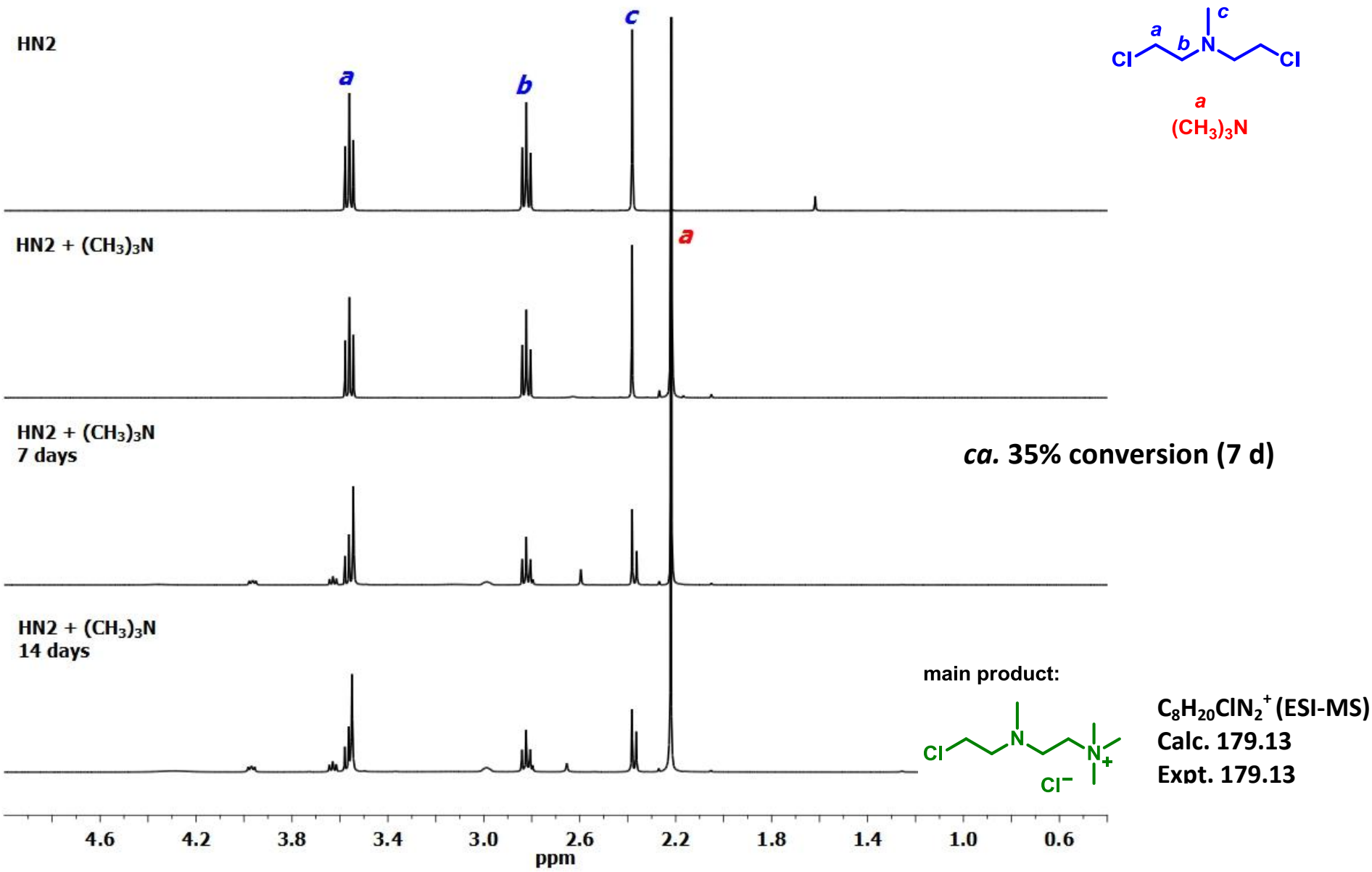

Figure S16. ^{1}H NMR monitoring (400 MHz, rt) of the reaction between HN2 and $(CH_3)_3N$ in $CDCl_3$ (with ESI-MS data).

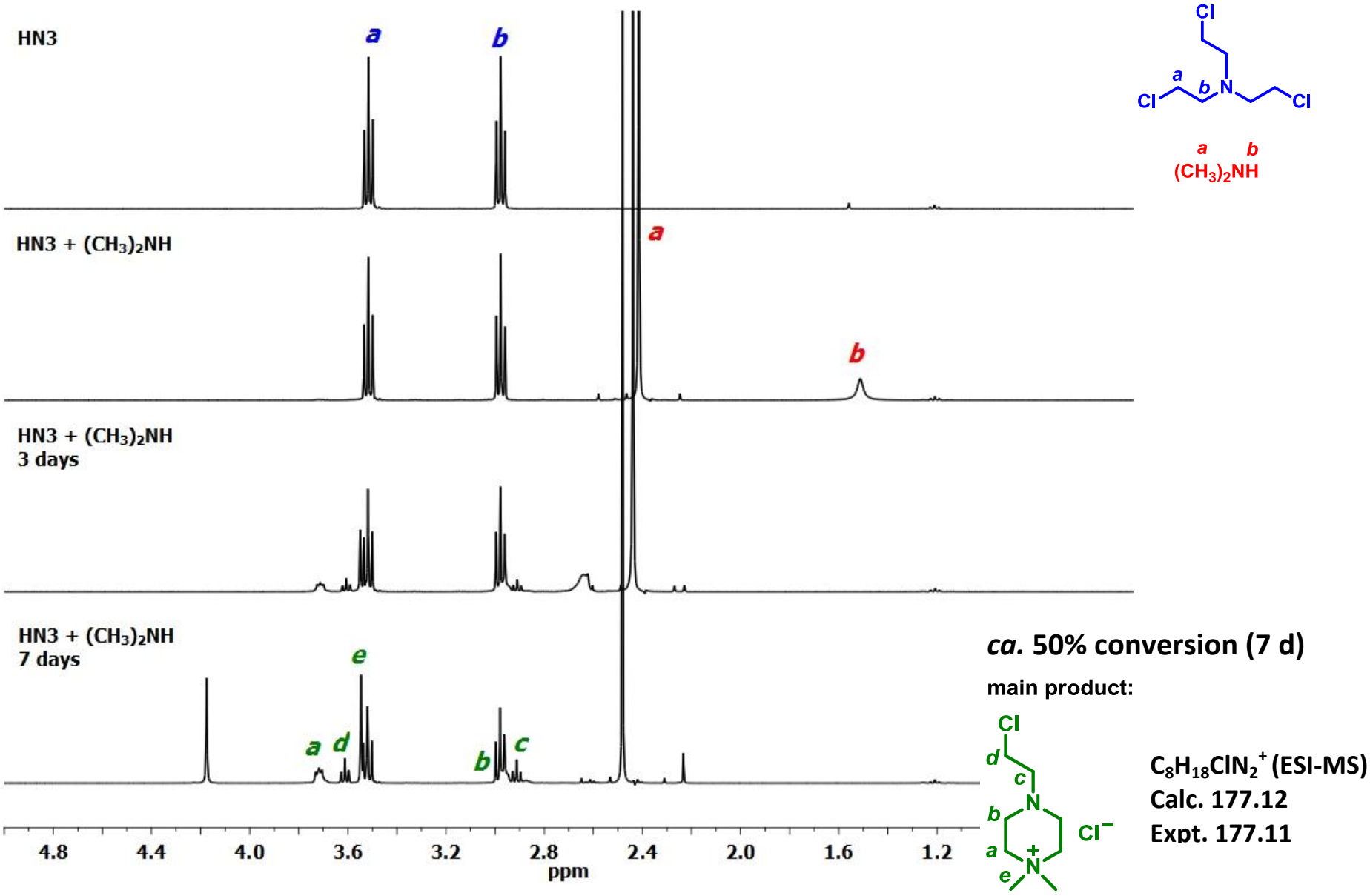

Figure S17. ^{1}H NMR monitoring (400 MHz, rt) of the reaction between HN3 and $(CH_3)_2NH$ in $CDCl_3$ (with ESI-MS data).

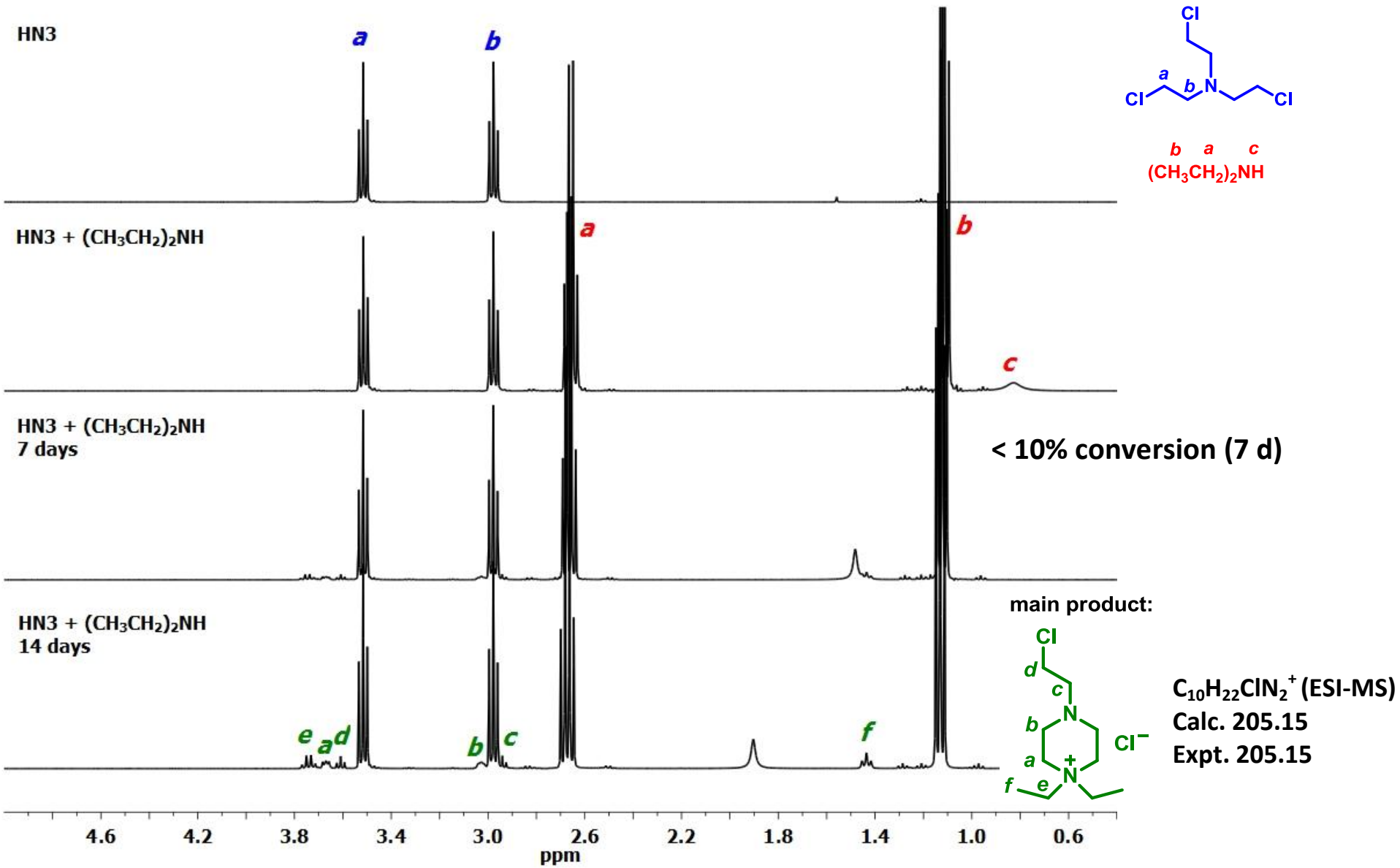

Figure S18. ^{1}H NMR monitoring (400 MHz, rt) of the reaction between HN3 and $(CH_3CH_2)_2NH$ in $CDCl_3$ (with ESI-MS data).

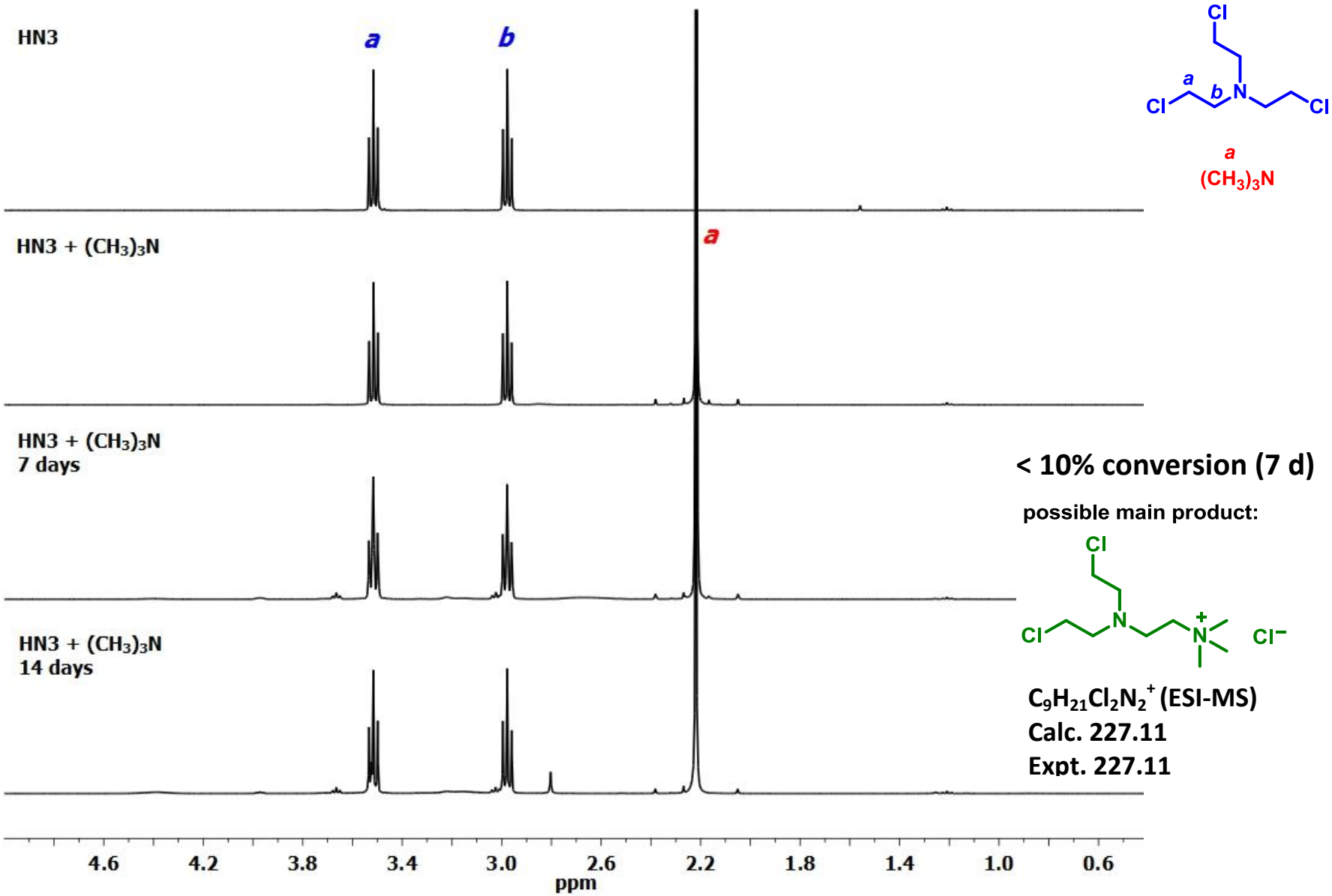

Figure S19. ^{1}H NMR monitoring (400 MHz, rt) of the reaction between HN3 and $(CH_3)_3N$ in $CDCl_3$ (with ESI-MS data).

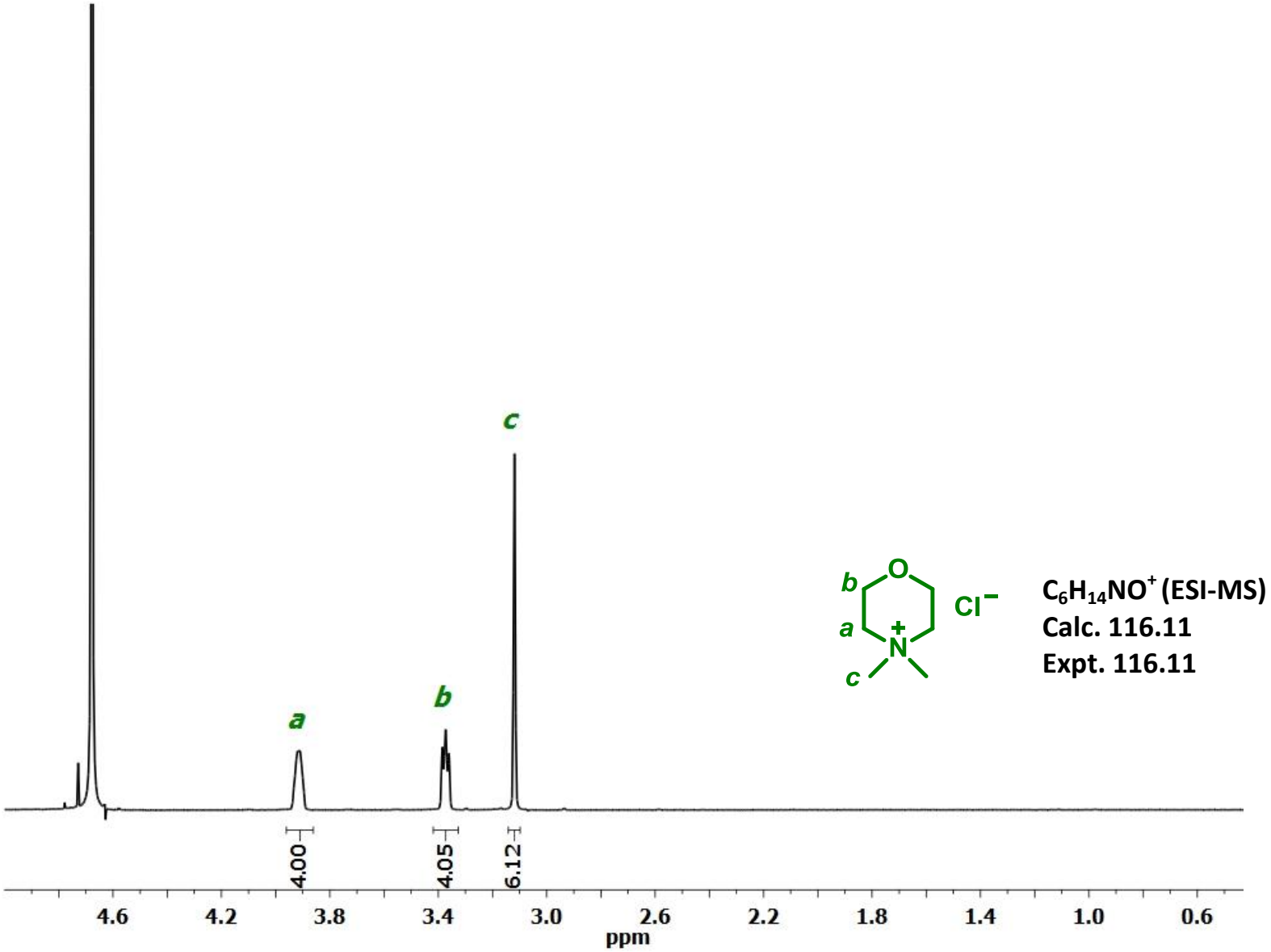

Figure S20. ^{1}H NMR (400 MHz, rt, D_2O) of the precipitates isolated from the reaction between BCEE and $(CH_3)_2NH$ in $CDCl_3$ (with ESI-MS data).

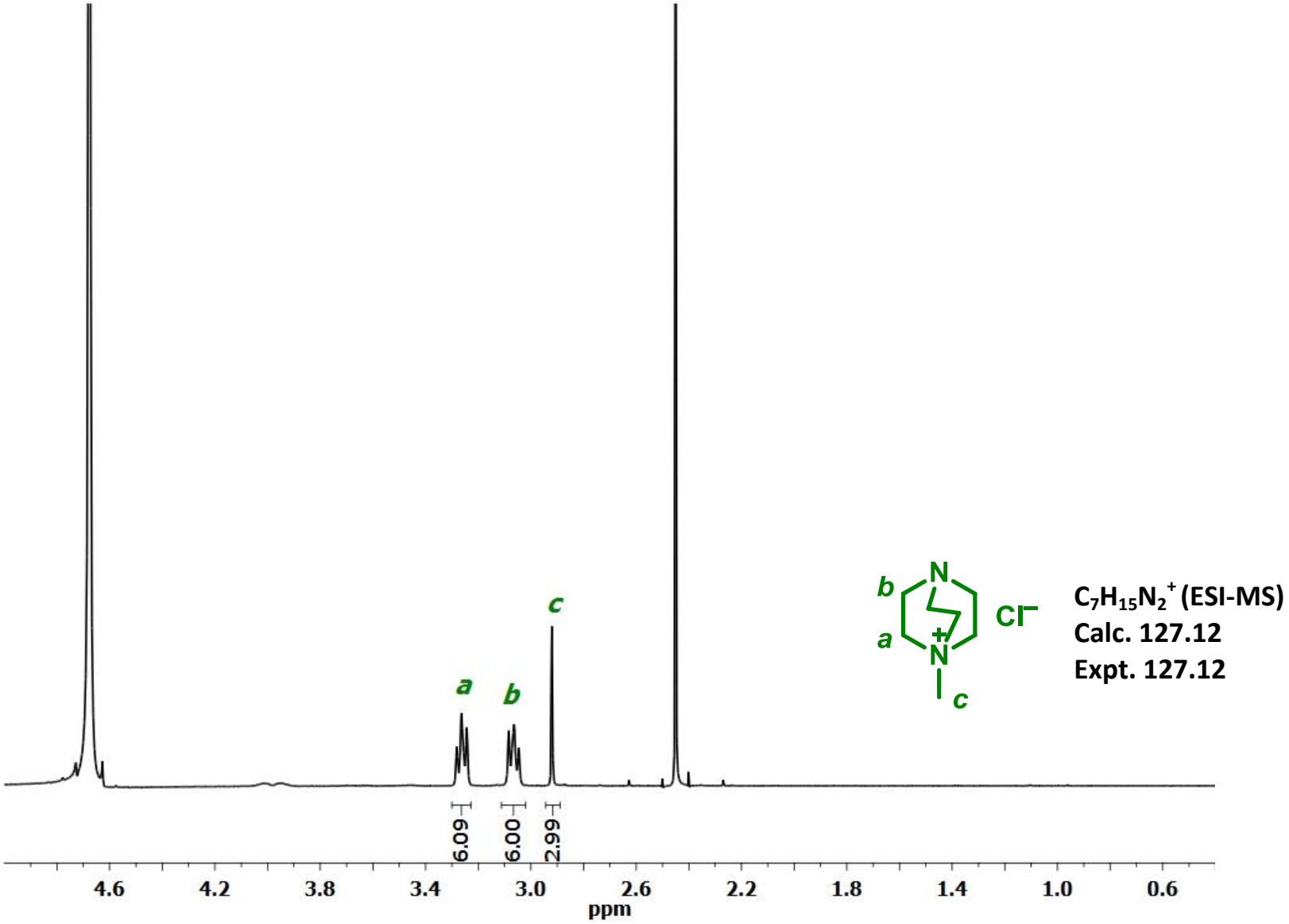

Figure S21. ^{1}H NMR (400 MHz, rt, D_2O) of the precipitates isolated from the reaction between HN3 and CH_3NH_2 in $CDCl_3$ (with ESI-MS data).

Table S1. Crystallographic data for 4,4-dimethylmorpholinium chloride (**A**) and 2,2'-oxybis(*N*,*N*,*N*-trimethylethanammonium) dichloride (**B**)

	A	**B**
Formula	$C_6H_{14}ClNO$	$C_{10}H_{28}Cl_2N_2O_2$
Formula weight	151.63	279.24
Crystal size (mm^3)	0.16×0.14×0.08	0.13×0.06×0.02
Crystal system	Orthorhombic	Monoclinic
Space group	$P2_12_12_1$	C_c
a (Å)	8.2735(3)	21.0466(7)
b (Å)	9.7455(4)	5.8427(2)
c (Å)	9.7543(4)	12.7574(4)
α (°)	90	90
β (°)	90	104.3700(10)
γ (°)	90	90
V ($Å^3$)	786.48(5)	1519.68(9)
Z	4	4
ρ_{calcd} (g cm^{-3})	1.281	1.221
λ (Å)	1.54178	1.54178
T (K)	100(2)	100(2)
F(000)	328	608
μ (mm^{-1})	3.695	3.777
Abs corr	Multi-scan	Multi-scan
Max, min trans	1.000, 0.817	1.000, 0.791
θ range (°)	6.42-69.35	4.34-69.06
Reflns collected	8137	4835
Indep reflns	1438	2177
R(int)	0.0223	0.0227
Data/restr/param	1438 / 0 / 140	2177 / 2 / 257
[a] R_1; wR_2	0.0154; 0.0418	0.0239; 0.0586
GOF (F^2)	1.154	1.096
Obsd data [I > 2σ(I)]	1438	2167
Largest diff. peak and hole (e $Å^{-3}$)	0.161, -0.135	0.272, -0.147

[a] R_1(obsd data) = $\Sigma \big| |F_o| - |F_c| \big| / \Sigma |F_o|$. wR_2 (all data) = $\{\Sigma [w(F_o^2-F_c^2)^2] / \Sigma [w(F_o^2)^2]\}^{1/2}$